Academic Journal of Science and Technology
ISSN: 2771-3032 | Vol. 14, No. 1, 2025

Dynamic Analysis of Load Distribution Optimization in Low-Speed Heavy-Duty Multi-Stage Planetary Gear System

Jinghao Sun, Wei Wu, Kaiqi Yan, Xincheng Zhao

School of Mechanical Engineering, Xi'an Shiyou University, Xi'an 710065, China

Abstract: A three-stage planetary gear reducer was designed for low-speed, heavy-load operating conditions, and a dynamic model was established after optimizing the load distribution through floating planet carriers. This model was used to study the nonlinear motion factors in the gear system, with a particular focus on the internal excitation caused by time-varying meshing stiffness. A mathematical analysis model of the mechanism was developed using MATLAB, and the time-varying meshing stiffness curves were derived. The analysis shows that the system exhibits periodic motion with changes in stiffness. Additionally, the load distribution of the system was analyzed based on stiffness variation, and the research indicates that as the stiffness increases, the transmission system experiences greater vibrations and impacts, leading to a decline in load distribution performance. Finally, a kinematic simulation model of the planetary gear system was established using ADAMS. Simulation results demonstrated that load distribution optimization for this transmission system is essential and provided the basis for this conclusion.

Keywords: Three-stage gear reducer; floating planet carrier; load distribution optimization; time-varying meshing stiffness, ADAMS.

1. Introduction

With the continuous progress and development of China's modern manufacturing industry, planetary gear transmissions have become an indispensable transmission form due to their high load capacity, compact structure, smooth transmission, and high efficiency. They are widely used in various mechanical fields, including the petroleum industry, lifting and transportation, construction machinery, aerospace, ships, high-speed trains, automobiles, and many industrial machines.

A multi-stage planetary gear transmission system is a complex mechanical power transmission system that exhibits both rigidity and flexibility. From a dynamic perspective, the gear transmission system is a continuous elastic system, where the system generates dynamic responses under internal and external excitations during motion, enabling power transmission. The internal excitation is a time-varying excitation generated by the meshing interaction between the gear pairs within the system, which is the key distinguishing factor of gear transmission systems compared to other mechanical transmission systems. Singh studied a single-stage planetary system, considering the effects of the sun gear support stiffness and the planet wheel needle bearing stiffness. Transmission system models with 4, 5, and 6 planet gears were established, highlighting that as the number of planet gears increases, the control range of the planet wheel pinhole positional error becomes smaller, and the system's load-sharing characteristics improve[1].Zhang DH, based on reliability theory and modern mechanical optimization design methods, optimized the volume, overlap degree, and efficiency of the NGW planetary gear transmission as objective functions. He then used ProE software to create a parametric solid model for assembly[2].Li Sheng et al. used the Gill integration method to solve the dimensionless motion equations of a two-stage planetary gear system in a milling cutter gearbox. They analyzed the effects of factors such as damping and excitation frequency on the system's bifurcation and chaotic characteristics[3].

This paper focuses on the planetary gear reducer used in the sugar production process for the pressing stage. A dynamic model of the system is established to study its nonlinear dynamic characteristics. The system's dynamic performance demonstrates the superiority of the optimized planetary gear reducer. The research results provide a theoretical foundation for the load-sharing optimization design of gear trains.

2. Modeling of the Planetary Gear Transmission System

2.1. Gear Train Parameter Configuration

The gearbox designed in this paper is applied to the sugar production process, with operating conditions in a low-speed, heavy-load environment. The motor power is 600 kW, the input speed ranges from 500 to 1200 r/min, and the gear ratio is approximately 150:1, with the expected output speed ranging from 0 to 10 r/min. After analysis, a multi-stage NGW planetary gear system was selected for the gearbox. The NGW system consists of a sun gear, a single set of planet gears, and a ring gear, using an internal meshing structure. This structure allows for a more compact gear arrangement while providing a wide range of transmission ratios, making it suitable for the required application. The motion schematic of the three-stage planetary gear reducer is shown, utilizing a three-stage 2K-H planetary gear system.

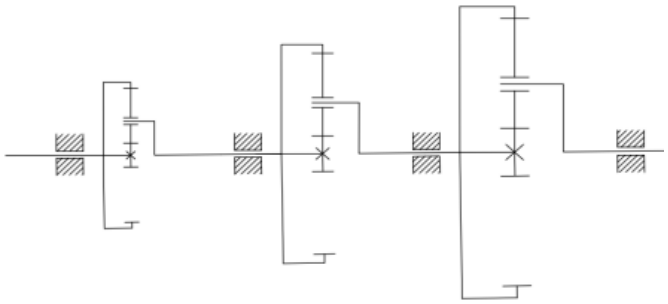

Figure 1. Schematic diagram of the motion of a three-stage planetary gear reduction gearbox

Finally, after applying the gear design standards, the parameters of the three-stage planetary gear reducer are presented in Table 1.

Table 1. Basic parameters of the planetary gear train

	Z	m_a	α	L	Number of gears	x_n
First-stage sun gear	**25**	**7**	**20**	**145**		**0.3387**
First-stage planet gear	**44**	**7**	**20**	**140**	**3**	**0.1872**
First-stage ring gear	**113**	**7**	**20**	**140**		**0.6820**
Second-stage sun gear	**18**	**14**	**20**	**200**		**0.3813**
Second-stage planet gear	**39**	**14**	**20**	**210**	**3**	**0.0701**
Second-stage ring gear	**96**	**14**	**20**	**210**		**0.5291**
Third-stage sun gear	**26**	**20**	**20**	**390**		**0.2641**
Third-stage planet gear	**28**	**20**	**20**	**400**	**3**	**0.2688**
Third-stage ring gear	**82**	**20**	**20**	**400**		**0.8017**

2.2. Load-sharing Structure Optimization of the Planetary Gear System

2.2.1. The Principle of Load Sharing.

Load power distribution refers to the process in which the n planet gears, uniformly distributed around the sun gear in a planetary gear system, share and transmit the load. From a theoretical perspective, the output power and load capacity of the transmission system are directly proportional to the number of planet gears. [4]When there is a change in the load distribution between the gear teeth, some components within the planetary gear system are allowed to float structurally, with the positions of the components optimized to restore a balanced load distribution. As illustrated, in a single-stage three-planet gear system, when the load is uniformly distributed among the planet gears, the load distribution generates a vector forming an equilateral triangle, which is the foundation of the load-sharing principle[5].

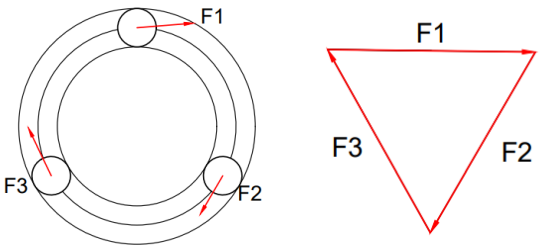

Figure 2. Load distribution diagram of the planetary transmission system

This paper employs the design of floating components within the gear train, primarily to facilitate practical manufacturing and assembly processes. The strategy is focused on minimizing the system's sensitivity to manufacturing and assembly tolerances, thereby indirectly improving the load-sharing performance of the planetary gear system[6].

Considering the low-speed operating conditions of the gearbox in this study, a floating planet carrier mechanism is implemented for the load-sharing system[7]. The shaft is coupled to the planet carrier via a dual-tooth coupling, which minimizes the need for excessive structural support, thereby facilitating the floating motion of the components. Additionally, the relatively large mass of the planet carrier itself ensures a stable floating motion, thereby maintaining operational stability and reducing dynamic fluctuations within the system.

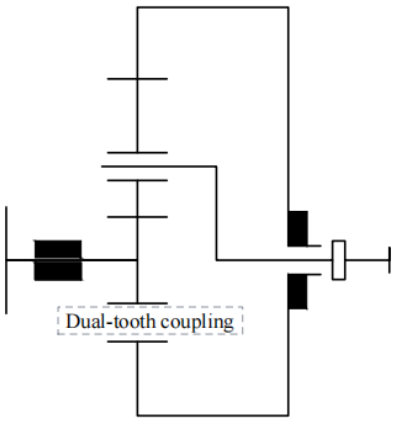

Figure 3. Schematic diagram of the floating motion of the planet carrier

The 3D model of the gear train after the planet carrier floating motion is shown in the figure 4 below. The sun gear is configured as a spline-shaft-gear component, with the sun gears connected via a coupling.

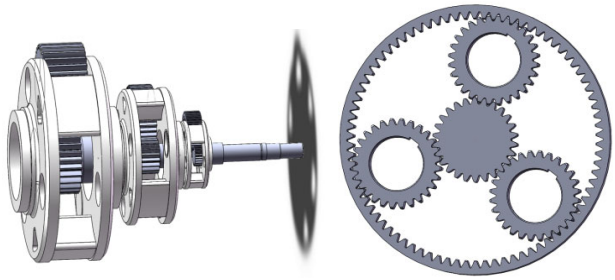

Figure 4. 3D model of the gear train

2.2.2. Load-Sharing Coefficient Calculation

To quantify the uniformity of load distribution in a planetary gear system, the load-sharing coefficient is a critical parameter used to assess the degree of load distribution between individual gears or components[8]. The load-sharing coefficient is defined by the following formula:

$$K_{H\beta} = \frac{\omega_{max}}{\omega_m} = \frac{(F_m)_{max}}{\frac{1}{n}\sum_{i=1}^{n} F_m} \tag{1}$$

In the formula, ω_{max} represents the maximum load per unit tooth width, ω_m represents the average load per unit tooth width, and $(F_m)_{max}$ denotes the maximum meshing force between the external meshing pairs of the n gears.

The load-sharing coefficients before and after the floating of the planet carrier, as calculated by the system of equations, are shown in the figure5.

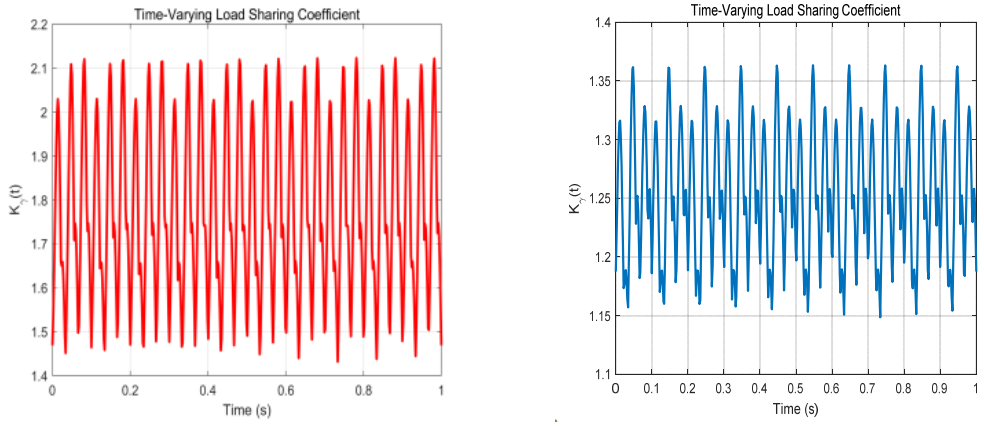

(a)Load-sharing coefficient without floating (b)Load-sharing coefficient with floating

Figure 5. Diagram of load-sharing coefficient variation

As illustrated in the diagram, the load-sharing coefficient of the transmission system with a floating planet carrier fluctuates around 1.23, whereas the original transmission system without a floating mechanism fluctuates around 1.79. A lower load-sharing coefficient signifies a more uniform distribution of the load among the planetary gears within the meshing pairs, thereby enhancing the load-sharing performance. The incorporation of a floating planet carrier significantly improves the load distribution uniformity in planetary gear systems, which is critical for reducing stress concentrations and extending the operational lifespan of the system.

3. Dynamic Analysis of the Gear Transmission System

3.1. Nonlinear Dynamics Analysis

In the dynamic analysis of gear systems, studying gear stiffness and internal excitation during meshing in multi-stage planetary gear systems are key research focuses .For the planetary gear system in this study, the energy method is used for calculation[9].The potential energy generated during meshing consists of five components[10]: shear potential energy U_s, Hertzian contact potential energy U_h, bending potential energy U_b, tooth base potential energy U_f, and compressive potential energy U_a. From the above potential energies, the shear stiffness k_s, Hertzian contact stiffness k_h,bending stiffness k_b,substrate deformation stiffness k_f,and axial compressive stiffness k_a can be calculated, as described by the following relationship:

$$\begin{cases} k_s = \dfrac{F^2}{2U_s} = \dfrac{F^2}{2\int_0^d \dfrac{1.2F_b^2}{2GA_x}dx} \\ k_b = \dfrac{F^2}{2U_b} = \dfrac{F^2}{2\int_0^d \dfrac{\left[F_b(d-x)-F_a h\right]^2}{2EI_x}dx} \\ k_a = \dfrac{F^2}{2U_a} = \dfrac{F^2}{2\int_0^d \dfrac{F_a^2}{2EA_x}dx} \\ k_f = \dfrac{F^2}{2U_f} \\ k_h = \dfrac{F^2}{2U_h} \end{cases} \tag{2}$$

In the formula, *h* is the distance from the centerline to the meshing point, *d* is the distance from the meshing point to the base circle, *E* is the Young's modulus, *G* is the shear modulus, I_x is the second moment of area of the gear tooth section at the base circle, A_x is the sectional area in the direction, F_a and F_b are the radial and tangential forces at the meshing point, respectively[11].

Additionally, from the geometric relationship of the involute curve and the diagram, it can be observed that:

$$\begin{cases} h = R_b\left[\left(\alpha_1+\varphi_b\right)\cos\alpha_1-\sin\alpha_1\right] \\ x = R_b\left[\cos\alpha+\left(\alpha_1+\varphi_b\right)\sin\alpha-\cos\varphi_b\right] \\ d = R_b\left[\cos\alpha_1+\left(\alpha_1+\varphi_b\right)\sin\alpha_1-\cos\varphi_b\right] \end{cases} \tag{3}$$

In the formula, α represents the pressure angle, R_b is the radius of the base circle, α_1 is the angle between the meshing force and the tooth's centerline, and φ_b is the half-arc angle of the base circle.

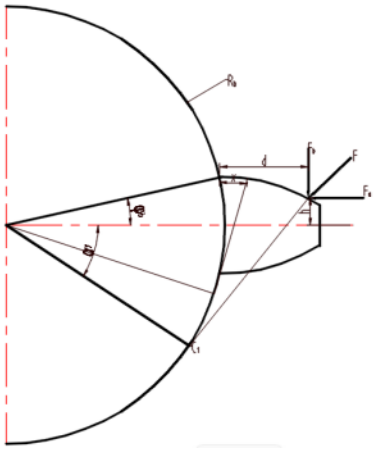

Figure 6. Straight gear tooth model

Using the above comprehensive equation, the different types of stiffness for an individual tooth pair can be determined.

$$\begin{cases} \dfrac{1}{k_h} = \dfrac{\pi EL}{4\left(1+\nu^2\right)} \\ \dfrac{1}{k_a} = \displaystyle\int_{-\alpha_1}^{\varphi_b} \frac{\left(\varphi_b-\alpha\right)\cos\alpha\sin^2\alpha_1}{2EL\left[\left(\varphi_b-\alpha\right)\cos\alpha+\sin\alpha\right]}da \\ \dfrac{1}{k_s} = \displaystyle\int_{-\alpha_1}^{\varphi_b} \frac{1.2\left(1+\nu\right)\left(\varphi_b-\alpha\right)\cos\alpha\cos^2\alpha_1}{EL\left[\left(\varphi_b-\alpha\right)\cos\alpha+\sin\alpha\right]}da \\ \dfrac{1}{k_b} = \displaystyle\int_{-\alpha_1}^{\varphi_b} \frac{3\left\{1+\cos\alpha_1\left[\left(\varphi_b-\alpha\right)\sin\alpha-\cos\alpha\right]\right\}^2\left[\left(\varphi_b-\alpha\right)\cos\alpha\right]}{2EL\left[\left(\varphi_b-\alpha\right)\cos\alpha+\sin\alpha\right]^3}da \\ \dfrac{1}{k_f} = \dfrac{\cos^2\alpha_1\left[L^*\left(\dfrac{u_f}{s_f}\right)^2+M^*\left(\dfrac{u_f}{s_f}\right)+P^*\left(1+Q^*\tan^2\alpha_1\right)\right]}{EL} \end{cases} \tag{4}$$

In the formula, E is the Young's modulus, ν is the Poisson's ratio, L is the tooth width, u_f is the distance from the meshing point to the tooth root circle's vertex, s_f is the arc length corresponding to the previous gear tooth on the tooth root circle, and L^* M^* P^* Q^* is the constant related to the ratio of the central angle of the corresponding gear to the pitch radius.

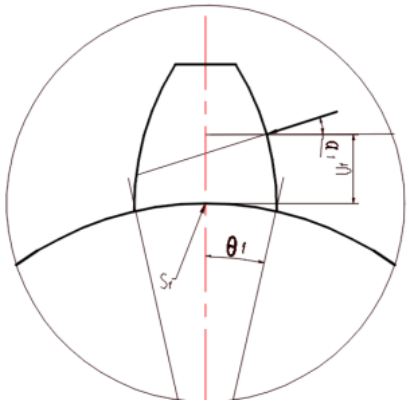

Figure 7. Substrate deformation geometric relationship

For gear systems with a contact ratio between 1 and 2, operating in a state of alternate single and double tooth meshing[12].the overall stiffness k of a single tooth pair can be expressed as:

$$k = \frac{F^2}{2U} = \frac{1}{\dfrac{1}{k_h}+\dfrac{1}{k_{s1}}+\dfrac{1}{k_{s2}}+\dfrac{1}{k_{b1}}+\dfrac{1}{k_{b2}}+\dfrac{1}{k_{f1}}+\dfrac{1}{k_{f2}}+\dfrac{1}{k_{a1}}+\dfrac{1}{k_{a2}}} \tag{5}$$

In the formula, F represents the contact force between the gear teeth, with subscripts 1 and 2 referring to the driving gear and the driven gear, respectively[13].

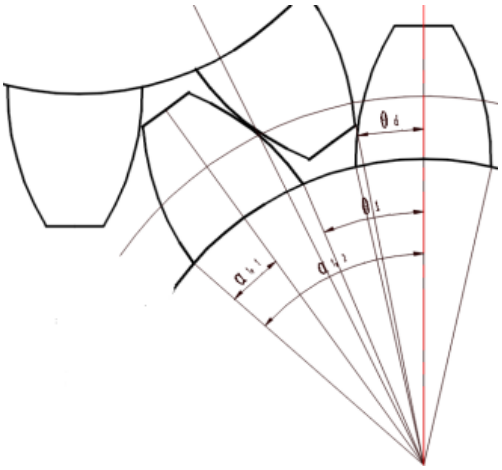

Figure 8. Gear double-tooth meshing motion relationship

The comprehensive stiffness of double-tooth meshing can be approximately analogized as the parallel connection of two springs, which is equivalent to the parallel connection of the stiffness of a single tooth pair[14].By summing the individual tooth stiffness expressions as outlined above, the comprehensive stiffness of double-tooth meshing can be expressed as:

$$k_z = \sum_{i=1}^{2} \frac{1}{\dfrac{1}{k_{h,i}}+\dfrac{1}{k_{b1,i}}+\dfrac{1}{k_{b2,i}}+\dfrac{1}{k_{s1,i}}+\dfrac{1}{k_{s2,i}}+\dfrac{1}{k_{a1,i}}+\dfrac{1}{k_{a2,i}}} \tag{6}$$

3.2. Calculation and Analysis of Time-varying Meshing Stiffness in Multi-stage Systems

By substituting the parameters of each stage gear into the comprehensive equation (4), the necessary data for

calculating various types of meshing stiffness are obtained.

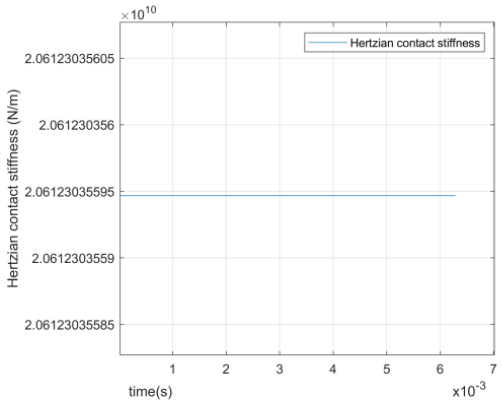

Figure 9. Hertzian contact stiffness

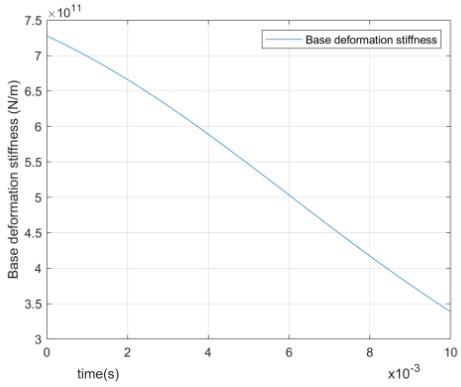

Figure 10. Variation curve of the sun gear base deformation stiffness

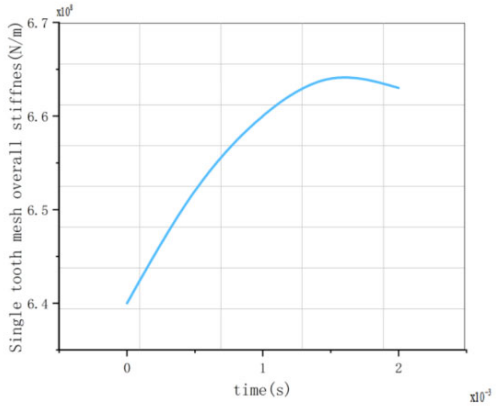

Figure 11. Single tooth mesh overall stiffness variation curve

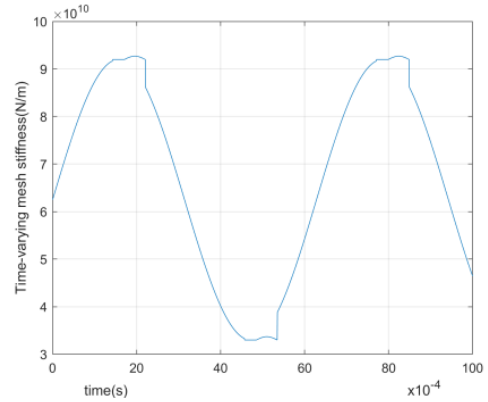

Figure 12 Time-varying mesh stiffness variation curve

3.3. The impact of time-varying meshing stiffness on load distribution in the gear train.

As shown in the figure, the time-varying meshing stiffness of the planetary gear system follows a simple harmonic motion function over time[15].indicating that the meshing stiffness consists of alternating components and an average component, as expressed by the following equation:

$$k_t = k_n + k_m \cos(\Omega\tau + \varphi) \tag{7}$$

In the formula, k_n is the average value of the time-varying meshing stiffness, k_m is the stiffness amplitude, Ω is the excitation frequency, and φ is the initial phase.

The ratio of k_m to k_n characterizes the temporal fluctuation of meshing stiffness. Thus, the meshing stiffness fluctuation coefficient is defined as:

$$G_k = \frac{k_m}{k_n} \tag{8}$$

By changing the meshing stiffness fluctuation coefficient while keeping other parameters constant, different values were used for calculations. The resulting load distribution coefficient for the planetary gear transmission system with a floating structure is shown in the figure13. As the fluctuation coefficient increases, the load distribution coefficient also increases. However, when the fluctuation coefficient reaches about 0.5 to 1, the growth of the load distribution coefficient slows down. This suggests that as stiffness increases, vibration amplitude increases, leading to greater vibrations and shocks, which reduces load distribution performance.

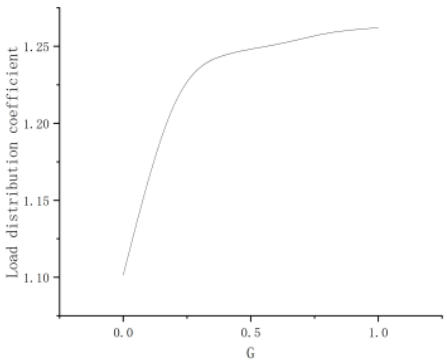

Figure 13. The relationship between load distribution coefficient and time-varying meshing stiffness

4. Kinematic Simulation Based on ADAMS

After constructing the 3D model in SolidWorks, it is imported into ADAMS, leaving only the kinematic meshing mechanism, as shown in the figure below. A separate simulation is performed for each stage of the gear system. The 3D model in Parasolid format is loaded into ADAMS, and the material properties of the components are defined according

to the design specifications. Then, constraints between the various components are established, as outlined in the following table:

Table 2. constraint conditions

	reference	Constraint
sun gear	ground	revolute pair
planet gear	ground	revolute pair
ring gear	ground	prismatic pair
planet carrier	ground	revolute pair
sun gear	planet carrier	prismatic pair

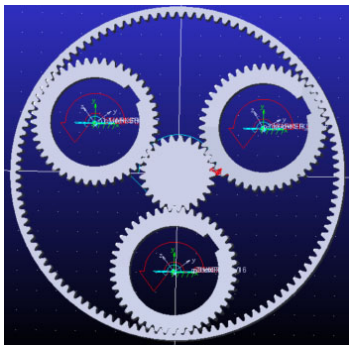

Figure14. Planetary Gear Train Simulation Structural Diagram

The contact force between gears is then defined, and the contact force is generally expressed by the following equation[12]:

$$F_N = \begin{cases} K \cdot \delta^{\varepsilon} + step(\delta, 0, 0, d_{max}, C_{max}) \dfrac{d\delta}{dt}, \delta \geq 0 \\ 0, \delta < 0 \end{cases} \quad (9)$$

In the equation, δ represents the actual contact distance between the two meshing gears,*d* is the penetration depth, C_{max} is the damping coefficient, and *step* is the step function.

From this equation, it is evident that contact force is generated only when the two gears collide. Therefore, the contact between the meshing pairs of gears is modeled using "entity-to-entity" collision contacts. The stiffness coefficient is selected, with the force exponent set to 2.2, damping set to 10 N·s/mm, static friction coefficient set to 0.3, dynamic friction coefficient set to 0.1, and pe0000000000netration depth set to 0.1 mm. Subsequently, the driving force and load are defined. The input speed is set to 1200 rpm, and the output speed is set to 8 rpm. A rotational drive is applied to the input gear, and a load in the opposite direction is applied to the fixed-axis gear.

Figure15. Set parameters

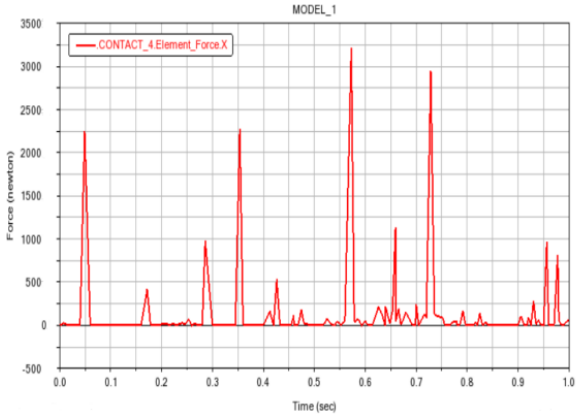

Figure16. Sun gear and planetary gear Contact force amplitude-frequency curve

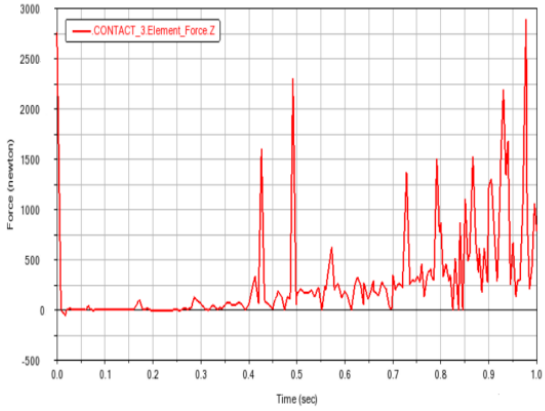

Figure 17. Planetary gear and ring gear Contact force amplitude-frequency curve

The simulation results indicate that the meshing force fluctuation between the sun gear and the planet gears is smaller than that between the planet gears and the internal gear. This difference is due to the centrifugal forces generated by the rotation of the planet gears, which are added to the force between the planet gears and the internal gear. Furthermore, as shown in the Figure16 and Figure17, both meshing pairs exhibit significant fluctuations, which implies considerable vibrations during the meshing process. These vibrations can have a substantial impact on the gear's lifespan, tooth surface strength, and other performance characteristics.

Additionally, the simulation of each stage of the planetary gear system shows that each stage experiences significant impacts. Therefore, it is necessary to implement load distribution optimization in the design to reduce the effects of these vibrations and improve the overall performance of the system.

5. Conclusion

(1) For planetary gear reducers in low-speed, heavy-load environments, a multi-stage planetary gear transmission system with a floating planet carrier configuration was established based on the original design. This system model facilitates smoother transmission, providing a theoretical foundation for the research and manufacturing of planetary gear transmission systems.

(2) Through nonlinear dynamic analysis of the planetary gear system and its meshing stiffness, the meshing motion was studied to obtain various time-varying meshing stiffness curves, which realistically reflect the actual motion of the

meshing pairs. The floating structure type significantly influences the load sharing performance of the planetary gear system. From the system analysis results of load sharing based on the stiffness of the floating components, it can be concluded that when manufacturing errors exist in the planetary gear system, the load-sharing coefficient with floating components is smaller than that without floating components. The load-sharing performance of the planetary gear system changes most rapidly with the variation of the floating components, while the change with meshing stiffness is relatively slower.

(3) The kinematic parameters obtained through the kinematic analysis of the gear system provide essential support for the optimization of structural parameters, enabling further optimization of the planetary gear reducer and improving design efficiency[17].This also lays the foundation for subsequent dynamic analysis as well as the analysis of gear friction and wear.

References

[1] Singh A. Load sharing behavior in epicyclic gears: Physical explanation and generalized formulation[J]. Mechanism & Machine Theory, 2010,45(3):511-530.

[2] Zhang DH, Wu FL, Zhang ST. et al. Application of improved genetic algorithm in reliability optimization design of NGW planetary gear transmission[J]. Journal of Mechanical Transmission, 2019, (10): 38-40.

[3] Li S , Wu QM, Zhang ZQ. Bifurcation and chaos analysis of multistage planetary gear train[J]. Nonlinear dynamics,2014, 75(1): 217-233.

[4] Le YX, Xiong XM, Wu H. Analysis and research of load sharing of planetary gear transmission based on flexible system[J]. Coal Mine Machinery, 2019, (10): 38-40.

[5] Peng B, Wang WK, Ma JX, et al. Co-dynamic simulation of Adams and Matlab for four-stage planetary hybrid reducer[J]. Machine Building & Automation, 2022, (03): 85-88+95.

[6] Liu XZ, Wu W, Wang L. et al. Optimization Design of Single-stage Planetary Gear Train Based on KISSsoft[J]. Mechanical & Electrical Engineering Technology, 2021, 50(03): 202-205+249.

[7] Li Y, Dong H, Luo YT. et al. Study on the time-varying meshing stiffness of a herringbone gear planetary transmission system with crack-pitting coupling[J]. Manufacturing Technology & Machine Tool, 2024, (11):41-47.

[8] Chen Q, Chang X. Optimization design for reliability of 3-stage planetary reducer of TBM[J], 2010,(24): 27-31.

[9] Wang YM, Qiu LJ, Li C, et al. Analysis of dynamic characteristic in the planetary gear transmission system of power split[J]. Ship Science and Technology, 2013, 35(11): 64-70.

[10] Li YP. Research on Dynamics Analysis Technology of Multi-Stage Planetary Gear Transmission System[D]. [S.l.]: Chinese Doctoral Dissertations Full-text Database, 2021.

[11] Shang P. Study on Design Technology and Load Sharing for High Reliability Planetary Gear Transmission[D]. [S.l.]: Chinese Doctoral Dissertations Full-text Database, 2009.

[12] Zhao Y. Dynamic Modeling and Analysis of High-Speed Flexible Planetary Gear Transmission System[D]. [S.l.]: Chongqing University, 2022.

[13] Wei W, Li YP, Yang YS. Dynamics simulation analysis of tooth root crack fault of planetary gearbox based on torsional vibration signal[J]. Journal of Mechanical Transmission, 2021, (10): 164-169.

[14] Wei J, Yang PW, Qin DT, et al. Equal Strength Optimal Design Method in Heavy-load Planetary Gear Transmission[J]. Journal of Beijing University of Technology, 2018, 44(07): 979-986.

[15] Li XM, Fu ZJ. Analysis of load sharing characteristics of gear reducer in large ships[J]. Ship Science and Technology, 2024, 46(20): 133-136.

[16] Xu XY, Yang W, Diao P. et al. Research of the dynamic load sharing of heavy load planetary gear system with multi-floating component[J].Journal of Mechanical Transmission, 2016, (12): 6-11.

[17] Tian D,Hu Y. Analysis and optimization design of support stiffness of floating components of wind turbine gearbox [J]. Acta Energiae Solaris Sinica, 2023, (04): 195-202